Structural determination of new solid solutions $[Y_{2-x}M_x][Sn_{2-x}M_x]O_{7-3x/2}$ (M = Mg or Zn) by Rietveld method

Mohamed Douma[1], El Hossain Chtoun[1], Raquel Trujillano[2], Vicente Rives[2,*]

[1]*Laboratoire de Chimie du Solide, Université Abdelmalek Essaâdi, Faculté des Sciences, B.P 2121, Tétouan, Morocco*

[2]*GIR-QUESCAT, Departamento de Química Inorgánica, Universidad de Salamanca, 37008, Salamanca, Spain*

Received 2 September 2010; received in revised form 25 November 2010; accepted 9 December 2010

Abstract

New $[Y_{2-x}M_x][Sn_{2-x}M_x]O_{7-3x/2}$ ($0 \leq x \leq 0.30$ for M = Mg and $0 \leq x \leq 0.36$ for M = Zn) solid solutions with the pyrochlore structure were synthesized via high-temperature solid-state reaction method. Powder X-ray diffraction (PXRD) patterns and Fourier transform infrared (FT-IR) spectra showed that these materials are new non-stoichiometric solid solutions with the pyrochlore type structure. The structural parameters for the solids obtained were successfully determined by Rietveld refinement based on the analysis of the PXRD diagrams. Lattice parameter (a) of these solid solutions decreases when x increases in both series. All samples obtained have the pyrochlore structure Fd-3m, no. 227 (origin at center -3m) with M^{2+} ($M = Mg^{2+}$ or Zn^{2+}) cations in Y^{3+} and Sn^{4+} sites, thus creating vacancies in the anionic sublattice.

Keywords: *oxides; inorganic compounds; chemical synthesis; X-ray diffraction*

I. Introduction

Synthetic pyrochlore-like solids are ternary metallic oxides with the general formula $A_2B_2O_7$ and structure similar to that of the natural mineral called pyrochlore with chemical formula $(NaCa)(NbTa)O_6F/(OH)$ [1]. The pyrochlore structure can be considered as an ordered, defective fluorite solid solution, as shown in Fig. 1. Cations A and B form a face centered cubic array, additionally ordered in the [110] directions and so A and B cations are eight- and six-coordinated, respectively, by oxygen anions, as described below.

The ideal cubic structure is highly symmetrical, with space group *Fd-3m* (no. 227). The general formula is $A_2B_2O_6O'$, and locating the origin on the B site [2], the ions occupy four crystallographically different sites (using Wyckoff's notation): A at 16d, B at 16c, O at 48f and O' at 8b. There is only one positional parameter, *x*, which describes the position of the oxygen atoms in the 48f site (*x*,1/8,1/8). The geometry of both the A and B cations depends on the value of the single variable oxygen positional parameter. The A cations have eight nearest neighbor anions forming a distorted cube; the B cations have six nearest neighbor oxygen ions forming a distorted octahedron. All oxygen ions lie within a tetrahedron of nearest neighbor cations. The 8b site has four A cations and the 48f site has two A and two B cations. The vacant 8a site has a tetrahedron of four B cations.

The cations at the A and B sites in the lattice can be replaced by other cations with different formal charge or different oxidation-reduction abilities, to synthesize various kinds of pyrochlore compounds with different physical or chemical properties.

Ternary tin oxides with the pyrochlore structure, $M_2Sn_2O_7$ (M = rare earth or yttrium), constitute a well-known series of compounds possessing SnO_6 octahedra. There are two main types of pyrochlore compounds: $A_2^{3+}B_2^{4+}O_7$ and $A_2^{2+}B_2^{5+}O_7$ [1]. Yttrium stannate ($Y_2Sn_2O_7$) has the $A_2^{3+}B_2^{4+}O_7$ structure and is significantly important because of its applications as ionic/electric conductors and because of its piezoelectricity, dielectric properties and resistance to radiation damage [3,4]. These materials have been widely used as catalysts, high-temperature pigment, electrochemical cells for NO_x decomposition, etc. [5–9].

* Corresponding author: tel: +34 923284489
fax: +34 923294574, e-mail: *vrives@usal.es*

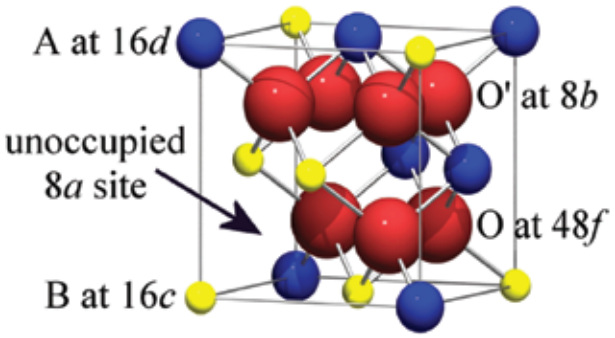

Figure 1. Unit cell of pyrochlore - blue spheres stand for A^{3+} cations, yellow ones for B^{4+} and red ones for O^{2-}

Due to their wide variety of compositions, some of the stannate pyrochlores exhibit a high efficiency for the oxidative coupling of methane and can be used as high-temperature gas sensors or fast ion conductors

[4]. Furthermore, stannate pyrochlores have been used as model compounds in MAS-NMR studies of paramagnetic solids [4]. Binary and ternary tin oxides have also been investigated as anode materials for lithium ion batteries (LIB) [10].

The structures of $[Eu_{2-x}M_x][Sn_{2-x}M_x]O_{7-3x/2}$ ($0 \le x \le 0.40$ for M = Mg and $0 \le x \le 0.45$ for M = Zn) solid solutions have been recently refined by Rietveld methods of X-ray diffraction [11,12]. Keeping in mind that changes in the composition of these kind of systems can regulate their structure and so their properties, we have synthesized two additional pyrochlore systems, namely $[Y_{2-x}M_x][Sn_{2-x}M_x]O_{7-3x/2}$ ($0 \le x \le 0.30$ for M = Mg and $0 \le x \le 0.36$ for M = Zn). The aim of present work is to study the effect of the substitution of large three or tetravalent cations by smaller divalent ones, Mg^{2+} and Zn^{2+}, on the pyrochlore structure. The structural study of the X-ray diffraction diagrams of both series has been performed by Rietveld analysis in order to obtain accurate data that are not currently available in the literature.

II. Experimental

$[Y_{2-x}M_x][Sn_{2-x}M_x]O_{7-3x/2}$ ($0 \le x \le 0.30$ for M = Mg and $0 \le x \le 0.36$ for M = Zn) were synthesized using the ceramic method in two steps as described in a previous paper [13]. Stoichiometric quantities of the oxides (Y_2O_3, SnO_2, MgO or ZnO, all reagents from Aldrich) were mixed and hand ground, then heated in air at 1000°C for 48 h and finally re-ground and submitted to calcinations at 1400°C for 96 h. The samples were heated at 2°/min and the cooling rate was 10°/min in both cases.

III. Data collection and Rietveld refinement

X-ray powder diffraction patterns were recorded in a Siemens D-500 diffractometer with a DACO-MP microprocessor using CuKα radiation (λ = 1.5405 Å). The powder diffraction diagrams were obtained by scanning with counting steps of 6 s from 2θ = 12° to 85° using 0.01° step-intervals. The PXRD obtained were analyzed by Rietveld method using Fullprof software [14], the atomic position set and the space group of the pyrochlore structure *Fd-3m*, no. 227 (origin at center -3m). A Pseudo-Voigt function was chosen to generate the line shape of the diffraction peaks. The background was estimated by linear interpolation between points corresponding to regions without reflections. A Rietveld refinement was performed to minimize the function $S_y = \sum_i w_i (y_i - y_{ci})^2$, where y_i and y_{ci} are the observed and calculated intensities at the i^{th} step and w_i is the weighting factor ($w_i = 1/y_i$). The following R factors were calculated: the profile factor $R_p = 100 \sum_i [|y_i - y_{ci}|/\sum_i |y_i|]$, the weighted profile factor $R_{wp} = 100[\sum_i w_i|y_i - y_{ci}|^2/\sum_i w_i|y_i|^2]^{1/2}$ and the Bragg factor, $R_{Bragg} = 100[\sum_i |I_i - I_{ci}|/\sum_i |I_i|]$, where I_i and I_{ci} are the observed and calculated integrated intensities, respectively.

The Fourier-transformed infrared (FT-IR) spectra were recorded in a Perkin-Elmer FT-IR-1600 spectrometer at a nominal resolution of 4 cm^{-1} and averaging 16 scans to improve the signal-to-noise ratio. Each sample was diluted in IR-grade potassium bromide and pressed into self-supported discs.

IV. Results and discussion

Table 1 shows the experimental and calculated results from X-ray Rietveld analysis of $Y_2Sn_2O_7$ and $[Y_{2-x}M_x][Sn_{2-x}M_x]O_{7-3x/2}$ (x = 0.154, M = Mg, Zn). The relative deviation between the experimental and calculated spacing is much lower than 0.9 %. These results confirm that the synthesized compounds are single phases as previously described in literature [13].

Similar compounds with formula $Eu_{1.78}Sn_{1.78}M_{0.44}O_{6.67}$ (M = Mg, Zn) showed a cubic pyrochlore structure with *Fd-3m* symmetry. The M^{2+} cations occupied the Eu and Sn sites according to $[Eu_{2-x}M_x][Sn_{2-x}M_x]O_{7-3x/2}$ (x = 0.22, M = Mg, Zn) [11,12]. Following this previous study, yttrium compounds with the formula $[Y_{2-x}M_x][Sn_{2-x}M_x]O_{7-3x/2}$ (x = 0.154, M = Mg, Zn) have been analyzed through Rietveld method.

Rietveld analysis could be applied to any of the compounds here prepared within the compositional domain where a stable, single phase is formed. However, our aim was to find a structural model suitable for all the chemical compositions within the stable structural domain with pure phases. Consequently, we have taken arbitrarily a sample with a given composition (but with a relatively large Mg or Zn content) and have applied our model until a satisfactory result is obtained, and the model is able to describe all solid solutions in the stable domain.

The structure of the new $[Y_{2-x}M_x][Sn_{2-x}M_x]O_{7-3x/2}$ (x = 0.154, M = Mg, Zn) compounds was refined from powder XRD data in a pyrochlore structure model, Y atoms at 16d (1/2,1/2,1/2), Sn atoms at 16c (0,0,0), O' atoms at 8b (3/8,3/8,3/8) and O atoms at 48f (x,1/8,1/8). The

Table 1. The experimental and calculated results for X-ray diffraction patterns of $Y_2Sn_2O_7$ and $[Y_{1.846}M_{0.154}][Sn_{1.846}M_{0.154}]O_{6.769}$ (M = Mg, Zn)

$Y_2Sn_2O_7$[a]			$Y_2Sn_2O_7$			$[Y_{1.846}Mg_{0.154}][Sn_{1.846}Mg_{0.154}]O_{6.769}$			$[Y_{1.846}Zn_{0.154}][Sn_{1.846}Zn_{0.154}]O_{6.769}$		
hkl	d_{cal} [Å]	I/I_0	*hkl*	d_{exp} [Å]	d_{cal} [Å]	I/I_0	*hkl*	d_{exp} [Å]	d_{cal} [Å]	I/I_0	*hkl*	d_{exp} [Å]	d_{cal} [Å]	I/I_0
111	5.9884	4.70	111	5.9814	5.9900	3.66	111	5.9804	5.9889	3.75	111	5.9798	5.9887	4.36
311	3.1273	4.50	311	3.1198	3.1282	5.50	311	3.1198	3.1276	5.50	311	3.1192	3.1275	6.04
222	2.9942	100	222	2.9867	2.9950	100	222	2.9871	2.9944	100	222	2.9887	2.9943	100
400	2.5930	27.62	400	2.5861	2.5937	28.78	400	2.5877	2.5932	28.50	400	2.5871	2.5931	29.77
511	1.9961	1.30	511	1.9924	1.9966	2.10	511	1.9913	1.9963	2.03	511	1.9906	1.9962	2.59
440	1.8335	43.44	440	1.8305	1.8340	48.66	440	1.8296	1.8337	46.88	440	1.8292	1.8336	49.48
622	1.5636	34.13	622	1.5618	1.5641	38.72	622	1.5611	1.5638	37.40	622	1.5608	1.5637	40.76
444	1.4971	7.10	444	1.4955	1.4975	8.48	444	1.4948	1.4972	8.05	444	1.4947	1.4971	9.25
800	1.2965	5.10	800	1.2956	1.2968	6.26	800	1.2951	1.2966	6.08	800	1.2950	1.2969	7.16
662	1.1897	11.51	662	1.1891	1.1901	14.18	662	1.1888	1.1898	13.28	662	1.1886	1.1898	15.42
840	1.1596	8.60	840	1.1591	1.1599	10.99	840	1.1588	1.1597	10.25	840	1.1585	1.1597	11.84
a = 10.3700 Å V = 1115.90 (Å)^3			a = 10.3751 (3) Å V = 1116.820 (4) (Å)^3				a = 10.3731 (1) Å V = 1116.161 (3) (Å)^3				a =10.3727 (7) Å V =1116.051 (6) (Å)^3			

[a]The standard XRD card: JCPDS 88-0445

Table 2. Refined atomic coordinates, occupancy and thermal parameters for $Y_2Sn_2O_7$ and the pyrochlore samples with $x = 0.154$

Phases	Atome	Site	x	y	z	Occupancy	B_{iso} [Å^2]
$Y_2Sn_2O_7$	Y	16d	1/2	1/2	1/2	1	0.548(8)
	Sn	16c	0	0	0	1	0.440(2)
	O	48f	0.3374(2)	1/8	1/8	1	1.299(4)
	O'	8b	3/8	3/8	3/8	1	0.776(8)
$[Y_{2-x}Mg_x][Sn_{2-x}Mg_x]O_{7-3x/2}$	Y	16d	1/2	1/2	1/2	0.928(5)	0.717(4)
	Mg_1	16d	1/2	1/2	1/2	0.071(4)	0.717(4)
	Sn	16c	0	0	0	0.917(4)	0.451(1)
	Mg_2	16c	0	0	0	0.082(5)	0.451(1)
	O	48f	0.3364(2)	1/8	1/8	0.961(6)	1.552(7)
	O'	8b	3/8	3/8	3/8	0.998(9)	0.642(4)
$[Y_{2-x}Zn_x][Sn_{2-x}Zn_x]O_{7-3x/2}$	Y	16d	1/2	1/2	1/2	0.919(1)	0.452(2)
	Zn_1	16d	1/2	1/2	1/2	0.081(1)	0.452(2)
	Sn	16c	0	0	0	0.927(1)	0.146(2)
	Zn_2	16c	0	0	0	0.073(1)	0.146(2)
	O	48f	0.3367(2)	1/8	1/8	0.962(1)	1.423(1)
	O'	8b	3/8	3/8	3/8	0.997(2)	0.451(2)

unique atomic coordinate is the x (48f) for oxygen atoms. This one varies from 0.3294 to 0.3397 over the series of stannate pyrochlores [15]. We have started with the value 0.33. Similar analysis has been performed for the $Y_2Sn_2O_7$ pyrochlore structure as a reference. As discussed in previous papers [11,12,16,17], we have placed the anionic vacancies in the 48(f) positions. For the 8(b) sites neither stable solutions nor good agreements factors were obtained.

Instrumental parameters were used to describe the profile: the zero-point in 2θ, background parameters, three peak-shape parameters, U, V and W in the formula $H^2 = U\tan^2\theta + V\tan\theta + W$ to describe a Pseudo-Voigt peak whose full width at half maximum, H, increases with θ_i. The structure parameters used were: a scale factor, the lattice constant, the positional coordinate, x, for O(48f), the occupancy factors (Table 2) of all atoms and the isotropic temperature factors.

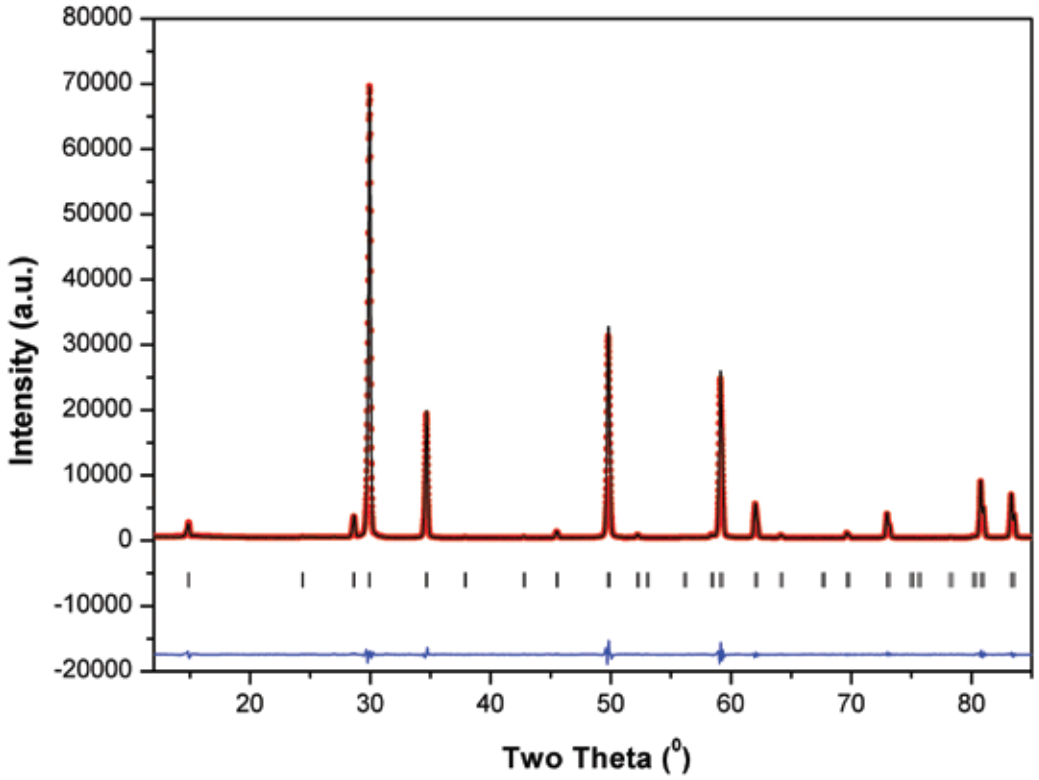

Figure 2. Observed (dots), calculated (solid line) and difference X-ray diffraction profiles for $[Y_{2-x}Mg_x][Sn_{2-x}Mg_x]O_{7-3x/2}$ ($x = 0.154$). Vertical marks correspond to the allowed reflections for the space group *Fd-3m*. The reliability *R*-factors obtained for this compound are: $R_p = 4.09\%$, $R_{wp} = 5.84\%$, $R_{Bragg} = 1.16\%$ and $\chi^2 = 5.29$ %.

Table 3. Experimental details and Refinement structural parameters for $Y_2Sn_2O_7$ and the samples with $x = 0.154$.

Data collection			
Powder diffractometer	Siemens D-500		
Radiation type; wavelength	CuKα; λ= 1.5405 Å		
2θ scan range	12–85°		
2θ step	0.01°		
Scan speed	6s/step		
Refinement program	Fullprof		
Rietveld refinements results			
Global formula	$Y_2Sn_2O_7$	$[Y_{2-x}Mg_x][Sn_{2-x}Mg_x]O_{7-3x/2}$	$[Y_{2-x}Zn_x][Sn_{2-x}Zn_x]O_{7-3x/2}$
Formula mass	527.19	499	511.66
Crystal system	Cubic	Cubic	Cubic
Space group	*Fd-3m*	*Fd-3m*	*Fd-3m*
Cell parameter [Å]	10.3751(3)	10.3731(1)	10.3727(7)
Cell volume [Å^3]	1116.820(4)	1116.161(3)	1116.051(6)
$x(O_{48f})$ parameter	0.3374(2)	0.3364(2)	0.3367(2)
Formula units per cell	Z=8	Z=8	Z=8
Peak shape function	Pseudo-Voigt	Pseudo-Voigt	Pseudo-Voigt
Selected contacts			
Sn-O [Å]	2.046(9)	2.041(5)	2.042(9)
Y-O [Å]	2.491(11)	2.497(11)	2.496(11)
Y-O' [Å]	2.246(4)	2.245(8)	2.245(7)
Sn-O-Sn [º]	127.34(4)	127.85(4)	127.75(4)
Y-O-Y [º]	94.82(5)	94.47(5)	94.54(5)
R_p [%]	3.70	4.09	4.09
R_{wp} [%]	5.27	5.84	5.47
R_{exp} [%]	2.73	2.68	2.62
R_{Bragg} [%]	0.91	1.16	1.70
χ^2 [%]	4.32	5.29	4.87

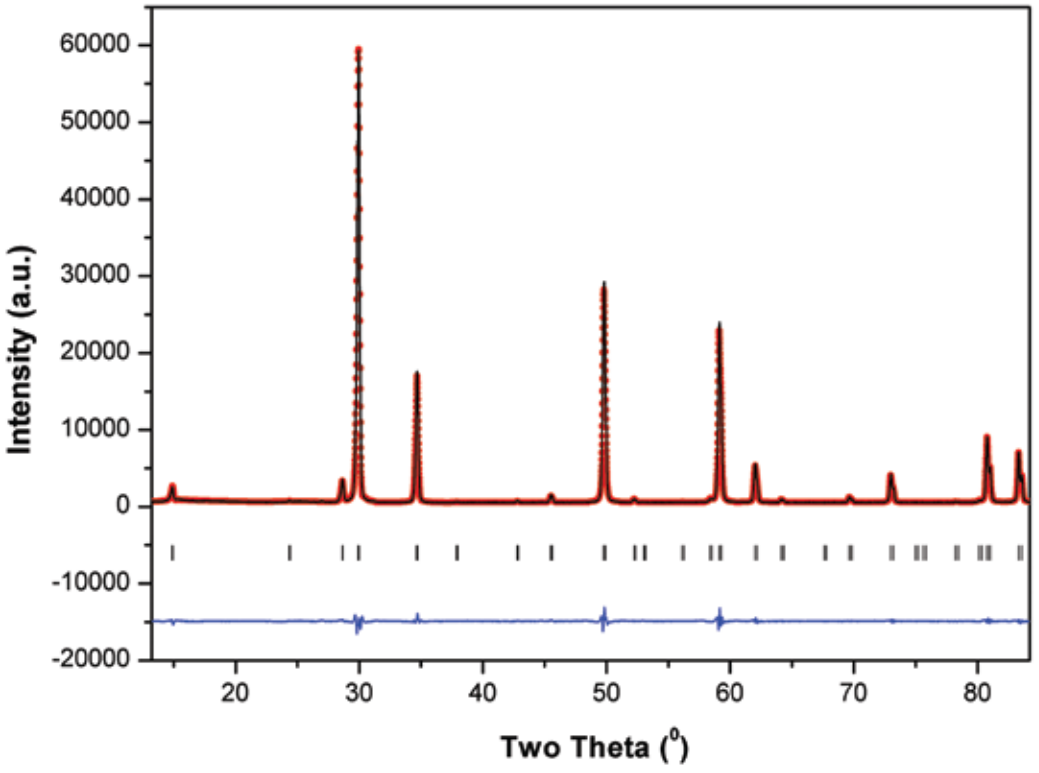

Figure 3. Observed (dots), calculated (solid line) and difference X-ray diffraction profiles for $[Y_{2-x}Zn_x][Sn_{2-x}Zn_x]O_{7-3x/2}$ ($x = 0.154$). Vertical marks correspond to the allowed reflections for the space group *Fd-3m*. The reliability *R*-factors obtained for this compound are: R_p = 4.09%, R_{wp} = 5.47%, R_{Bragg} = 1.70% and χ^2= 4.87 %

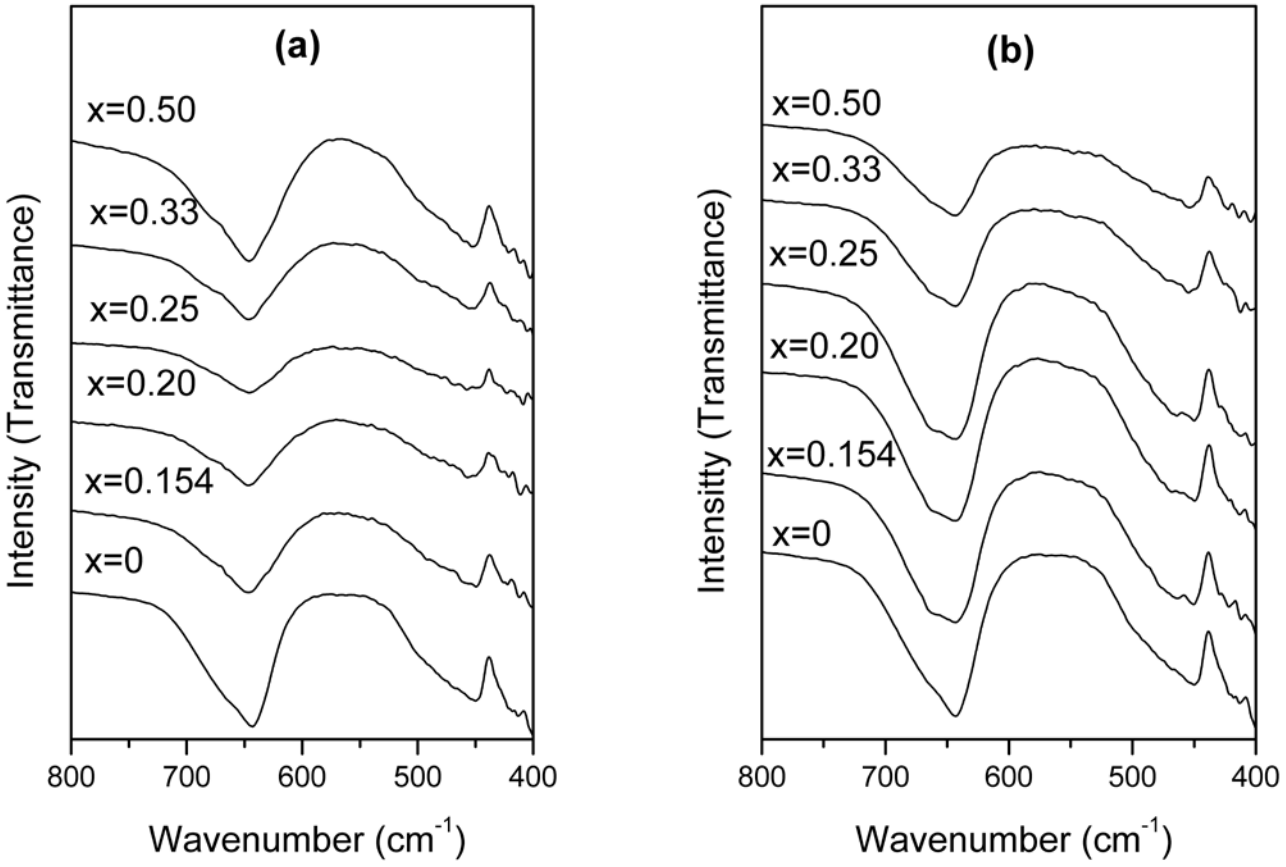

Figure 4. FT-IR spectra of: a) $[Y_{2-x}Zn_x][Sn_{2-x}Zn_x]O_{7-3x/2}$; b) $[Y_{2-x}Mg_x][Sn_{2-x}Mg_x]O_{7-3x/2}$.

Fig. 2 shows a typical plot of observed, calculated, and difference profiles for $[Y_{2-x}M_x][Sn_{2-x}M_x]O_{7-3x/2}$ (x = 0.154, M = Mg), while Fig. 3 shows the plot corresponding to $[Y_{2-x}M_x][Sn_{2-x}M_x]O_{7-3x/2}$ (x = 0.154, M = Zn). In all cases, the agreement between the observed and calculated profiles is excellent and the final R factors are satisfactory and good, particularly for R_B factors which depend on both the atomic coordinates and the chemical composition. These fits between calculated and observed intensity provided the structural parameters shown in Table 3. Data in Figs. 2 and 3 and Table 3 reveal the characteristic reflections (h k l) for $Y_2Sn_2O_7$ (JCPDS 88-0445), such as (111), (311), (222), (400), (511), (440), (622), (444), (800), (662) and (840), and that the value of the lattice parameter of $[Y_{2-x}M_x][Sn_{2-x}M_x]O_{7-3x/2}$ (x = 0.154, M = Mg, Zn) is close to that of $Y_2Sn_2O_7$. This demonstrates that $[Y_{2-x}M_x][Sn_{2-x}M_x]O_{7-3x/2}$ (x = 0.154, M = Mg, Zn) must possess the pyrochlore structure. The lattice parameter a decreases gradually from $Y_2Sn_2O_7$ to $[Y_{2-x}M_x][Sn_{2-x}M_x]O_{7-3x/2}$ (x = 0.154, M = Mg) and to $[Y_{2-x}M_x][Sn_{2-x}M_x]O_{7-3x/2}$ (x = 0.154, M = Zn). The average effective ionic radii for Mg^{2+} (0.805 Å) and Zn^{2+} (0.820 Å), calculated as $[x{\cdot}r(M^{2+})_{[8]} + x{\cdot}r(M^{2+})_{[6]}]/2x$ (with x = 0.154, $r(Mg^{2+})_{[8]}$ = 0.89 Å, $r(Mg^{2+})_{[6]}$ = 0.72 Å, $r(Zn^{2+})_{[8]}$ = 0.9 Å and $r(Zn^{2+})_{[6]}$ = 0.74 Å) are slightly smaller than that of Y^{3+} and Sn^{4+} ions (0.854 Å) in $Y_2Sn_2O_7$, calculated according to $[2{\cdot}r(Y^{3+})+2{\cdot}r(Sn^{4+})]/4$ [18]; hence, the substitution of M^{2+} ions for Y^{3+} and Sn^{4+} ions decreases the lattice parameter. These characteristic diffractions indicate that the M (Mg, Zn) metal cations are well distributed in the pyrochlore structure and a small concentration of the doped ions in the pyrochlores does not change the crystal purity since there is no diffraction maximum related with other crystalline compounds. The formation of the solid solutions corresponds to the substitution of M^{2+} (Mg^{2+} or Zn^{2+}) for Y^{3+} and Sn^{4+} ions with the simultaneous developing of anionic vacancies in the 48(f) positions.

It has been observed from Rietveld analysis that when the concentration of M (Mg^{2+} or Zn^{2+}) in $[Y_{2-x}M_x][Sn_{2-x}M_x]O_{7-3x/2}$ increases, the value of the x parameter of the 48f oxygen changes from 0.3374 (for $Y_2Sn_2O_7$) to 0.3364 (for M = Mg) and to 0.3367 (for M = Zn). In the pyrochlore structure, the 8a position is vacant; therefore, the 48f oxygen shifts from its ideal tetrahedral position towards two of its surrounding B cations. The t shift is correlated to the x coordinate of 48f oxygen atoms by the relationship x = 6/16–t. For the solid solution $[Y_{2-x}M_x][Sn_{2-x}M_x]O_{7-3x/2}$ (M = Mg, Zn) the lower charged cations M^{2+} substitute the Y^{3+} and Sn^{4+} cations; as a consequence, an increase of the t shift and a decrease of the x positional parameter takes place (Table 3). Ideally, in an ordered pyrochlore structure ($A_2B_2O_6O'$), the oxygen x parameter lies within the limit 0.3125–0.375 if taking the origin (0,0,0) at the B cation site [1].

The FT-IR spectra were recorded on polycrystalline powders in the form of KBr discs from 4000 to 400 cm^{-1}. There are seven characteristic absorption bands in the region 1200–100 cm^{-1} for the pyrochlore compounds with the formula $A_2B_2O_7$ [19] but those below 400 cm^{-1} cannot be recorded with our instrument. Fig. 4 shows the FT-IR spectra of $[Y_{2-x}M_x][Sn_{2-x}M_x]O_{7-3x/2}$ ($0 \le x \le 0.30$ for M = Mg and $0 \le x \le 0.36$ for M = Zn) in the 800–400 cm^{-1} range. This figure includes also the spectrum of the sample with $x = 0.5$ to demonstrate the differences in the spectra when segregation of a new phase (MgO or ZnO) occurs from pyrochlore. The strong band in the region of 750–580 cm^{-1} can be ascribed to Sn-O stretching vibration [1]. All spectra are similar to that of the $Y_2Sn_2O_7$ pyrochlore, no displacements can be observed in the spectra, thus suggesting that the M^{+2} (M = Mg, Zn) metal cations are well distributed in the pyrochlore structure.

V. Conclusions

A new pyrochlore solid solution with formula $[Y_{2-x}M_x][Sn_{2-x}M_x]O_{7-3x/2}$ ($0 \le x \le 0.30$ for M = Mg and $0 \le x \le 0.36$ for M = Zn) was synthesized by solid-state reaction. The incorporation of M^{2+}(Mg^{2+}, Zn^{2+}) into the yttrium stannate pyrochlore $Y_2Sn_2O_7$ induced the decrease of lattice parameter with x while remaining the cubic pyrochlore phase. Rietveld refinements achieved for $[Y_{2-x}M_x][Sn_{2-x}M_x]O_{7-3x/2}$ ($x = 0.154$, M = Mg, Zn) compounds confirmed an overall $Y_2Sn_2O_7$ cubic pyrochlore structure with M^{2+} cations in both Y and Sn sites and simultaneously creation of vacancies in the anionic sublattice. Bands recorded in the infrared spectra of all the compounds are characteristic of the pyrochlore structure.

Acknowledgements: Authors acknowledge financial support from AECI for the PCI (España-Mediterráneo) project. M. Douma acknowledges a MAEC-AECID grant.

References

1. M.A. Subramanian, G. Aravamudan, G.V. Subba Rao, "Oxide pyrochlores - A review", *Prog. Solid State Chem*., **15** (1983) 55–143.
2. A.M. Srivastava, "Chemical bonding and crystal field splitting of the Eu^{3+} $^7F_1$ level in the pyrochlores $Ln_2B_2O_7$ (Ln = La^{3+},Gd^{3+}, Y^{3+}, Lu^{3+}; B = Sn^{4+}, Ti^{4+})", *Opt. Mater*., **31** (2009) 881–885.
3. K.E. Sickafus, L. Minervini, R.W. Grimes, J.A. Valdez, M. Ishimaru, F. Li, K.J. McClellan, T. Hartmann, "Radiation tolerance of complex oxides" *Science*, **289** (2000) 748–751.
4. Z.J. Chen, H.Y. Xiao, X.T. Zu, L.M. Wang, F. Gao, J. Lian, R.C. Ewing, "Structural and bonding properties of stannate pyrochlores: a density functional theory investigation", *Comput. Mater. Sci*., **42** (2008) 653–658.
5. H. Zhu, D. Jin, L. Zhu, H. Yang, K. Yao, Z. Xi, "A general hydrothermal route to synthesis of nanocrystalline lanthanide stannates: $Ln_2Sn_2O_7$ (Ln =Y, La–Yb)", *Alloys Compd*., **464** (2008) 508–513.
6. S. Park, H.J. Hwang, J. Moon, "Catalytic combustion of methane over rare earth stannate pyrochlore", *Catal. Lett*., **87** [3-4] (2003) 219–223.
7. D.J. Haynes, A. Campos, D.A. Berry, D. Shekhawat, A. Roy, J.J. Spivey, "Catalytic partial oxidation of a diesel surrogate fuel using an Ru-substituted pyrochlore", *Catal. Today*, **155** [1-2] (2010) 84–91.
8. D.J. Haynes, D.A. Berry, D. Shekhawat, J.J. Spivey, "Catalytic partial oxidation of n-tetradecane using pyrochlores: Effect of Rh and Sr substitution", *Catal. Today*, **136** [3-4] (2008) 206–213.
9. S. Park, H.S. Sony, H.J. Choi, J. Moon, "NO decomposition over the electrochemical cell of lanthanum stannate pyrochlore and YSZ composite electrode", *Solid State Ionics*, **175** (2004) 625–629.
10. N. Sharma, G.V. Subba Rao, B.V.R. Chowdari, "Anodic properties of tin oxides with pyrochlore structure for lithium ion batteries", *J. Power Sources*, **159** (2006) 340–344.
11. M. Douma, E.H. Chtoun, R. Trujillano, V. Rives, "X-ray Rietveld analysis and Fourier transform infrared spectra of the solid solutions $[Eu_{2-x}M_x][Sn_{2-x}M_x]O_{7-3x/2}$ (M = Mg or Zn)", *Mater. Res. Bull*., **45** (2010) 29–33.
12. R. Trujillano, M. Douma, E.H. Chtoun, V. Rives, "Crystallographic study by X-ray Rietveld analysis of new synthetic pyrochlores $[Eu_{2-x}M_x][Sn_{2-x}M_x]O_{7-3x/2}$ (M = Mg or Zn)", *Macla*, **11** (2009) 187–188.
13. M. Douma, E.H. Chtoun, R. Trujillano, V. Rives, S. Khayroun., "Synthèse et étude radiocristallographique de nouvelles solutions solides de estructure pyrochlore $(1-x)A_2Sn_2O_7$ -xMO (A=Eu, Y, M=Mg, Zn)", *Ann. Chim. Sci. Mater*., **34** (2009) 21-26.
14. J. Rodriguez-Carvajal, pp.127 in XV *Conference of International Union of Crystallography*, Toulouse 1998.
15. B.J. Kennedy, B.A. Hunter, C.J. Howard, "Structural and bonding trends in tin pyrochlore Oxides", *J. Solid State Chem*., **130** [1] (1997) 58–65.
16. E. Chtoun, L. Hanebali, P. Garnier, J.M. Kiat, "X-Rays and neutrons rietveld analysis of the solid solutions $(1-x)A_2Ti_2O_7$-xMgTiO$_3$ (A = Y or Eu)" *Eur. J. Solid State Inorg. Chem*., **34** [6] (1997) 553–561.
17. E. Chtoun, L. Hanebali, P. Garnier, "Synthesis and X-ray diffractometric studies of $(1-x)A_2Ti_2O_7$ - xFe$_2$TiO$_5$ (A= Eu, Y) solid solutions", *Ann. Chim. Sci. Mater*., **26b** (2001) 27–32.
18. X.L. Li, Y.W. Song, H. Xiong, Y.Q. Jia, N. Matsushita, Y. Xuan, "Synthesis, crystal structure and magnetic property of $Sm_{2-x}Co_xTi_{2-x}Nb_xO_7$ ($x = 0$, 0.2, 0.4) ", *Mater. Chem. Phys.*, **77** (2002) 625–631.
19. T.T. Zhang, K.W. Li, J. Zeng, Y.L. Wang, X.M. Song, H. Wang, "Synthesis and structural characterization of a series of lanthanide stannate pyrochlores", *J. Phys. Chem. Solids*, **69** (2008) 2845–2851.